Research Article | Vol. 14, No. 1 / 1 Jan 2024 / Optical Materials Express 226
Optical Materials EXPRESS

Effect of the nanopillar diameter on diamond silicon vacancy center spin lifetime

T. Lutz,[1,*] T. Masuda,[1] J. P. Hadden,[2] I. Fescenko,[3,4] V. M. Acosta,[3] W. Tittel,[1,5,6] and P. E. Barclay[1]

[1]University of Calgary, Institute for Quantum Science and Technology and Department of Physics and Astronomy, 2500 University Drive NW, Calgary, Canada
[2]School of Engineering, Cardiff University, Queen's Buildings, The Parade, Cardiff, CF24 3AA, United Kingdom and Translational Research Hub, Maindy Road, Cardiff, CF24 4HQ, United Kingdom
[3]University of New Mexico, Center for High Technology Materials and Department of Physics and Astronomy, Albuquerque, USA
[4]Laser Center, University of Latvia, Riga, LV-1004, Latvia
[5]Department of Applied Physics, University of Geneva, Switzerland
[6]Constructor University, Bremen, Germany
[*]pbarclay@ucalgary.ca

Abstract: Color centers in diamond micro and nano-structures play an important role in a wide range of quantum technologies. However, obtaining high-quality color centers in small structures is challenging, as properties such as spin population lifetimes can be affected by the transition from a bulk to nanostructured crystal host. In this manuscript, we measure how population lifetimes of silicon vacancy center orbital states change when they are created in nanopillars whose diameters vary from 1 μm to 120 nm. We also discuss the influence of annealing methods on the silicon vacancy inhomogeneous linewidth. After selecting a sample with low inhomogeneous broadening and patterning it with nanopillars, we expected that restricted vibrational modes in the smallest structures could extend spin population lifetimes. However, we found that this effect was masked by other effects that reduced population lifetimes, suggesting that imperfections in the crystal lattice or surface damage caused by etching can influence SiV spins.

1. Introduction

Color centers in diamond are used for a broad variety of applications such as sensing [1,2], hybrid quantum optomechanics [3–6] and quantum information processing [7–14]. Many of these applications require color centers implanted [15,16] within micro or nano structures [17,18] that are engineered to modify the optical [19] or phononic density of states [20] while requiring color centers that are stable in their emission wavelength. This latter property is particularly important in order to use color centers as sources of indistinguishable photons [21,22] in quantum networking applications, and demands that they have narrow inhomogeneous broadening. However, there are few systematic studies on how the transition from bulk to the nanoscale influences the above mentioned spectroscopic properties reported for color centers in nanostructured diamond.

Among the numerous diamond color centers, the negatively charged silicon-vacancy center (SiV) has received significant attention [23–31] due to its favorable spectroscopic properties [32] that make it appealing for the above mentioned applications. Its atomic inversion-symmetry makes it less susceptible to spectral diffusion compared to the nitrogen-vacancy (NV) center, and more than 80% of its emission is contained in its zero phonon line [33]. However, SiV electronic spin coherence is strongly affected by phonons [34], requiring operation at ultralow temperature for many quantum related applications [35]. Nanoscale strain engineering can extend the SiV spin lifetimes by modifying its electronic spin transitions [25,36], and suspended phononic crystals have been predicted [20] and recently demonstrated [37,38] to allow SiV spin properties to be

#503513 https://doi.org/10.1364/OME.503513
Journal © 2024 Received 17 Aug 2023; revised 28 Oct 2023; accepted 30 Oct 2023; published 21 Dec 2023

Optical Materials EXPRESS

enhanced. Similarly, SiV centers localized in diamond nanoparticles have been observed to possess extended spin orbital lifetime due to modifications of phononic density of states by their 20 – 50 nm diameter crystal size [39]. A natural question is whether similar spin enhancements are possible by patterning bulk diamond substrates with supported nanoscale structures such as well studied diamond nanopillars [18] that possess restricted phononic density of states [20].

In this work we study the optical and spin properties of SiV color centers hosted in diamond nanopillars whose dimension vary from the microscale to the nanoscale. We begin by creating SiV color centers by ion implantation and annealing of several diamond samples. We then measure differences in their optical properties and investigate to what degree thermal annealing can alter SiV inhomogeneous optical linewidth. We find that despite efforts to follow identical implantation and annealing recipes between samples, the SiV inhomogenous linewidth can varying significantly and that re-annealing was not found to reduce the inhomogeneous broadening. After selecting a sample with low inhomogeneous broadening, we investigate how the SiV orbital state lifetime changes when the diamond host crystal is patterned and etched to create nanopillars of varying diameter. We observe that orbital state lifetimes tend to decrease in the smallest nanostructures rather than increase due to a theoretically predicted suppression of resonant vibrational modes. Further investigation is required to isolate the mechanism responsible for this behavior. We believe that these studies will also be relevant to other group-IV color centers such as the SnV [40].

2. Sample preparation and characterization

The diamond samples studied here were purchased from Element Six and are nominally identical, with the following specifications: $3\times3\times0.5$ mm electronic grade diamond chips (typical nitrogen concentration of $10^{13}/\text{cm}^3$ and NV concentration of 10^{10} – $10^{11}/\text{cm}^3$), polished on both sides. The low NV concentration is required since the presence of many NVs in the sample can mask the SiV signal. The samples were cleaned using a mixture of perchloric, nitric, and sulphuric acid (1:1:1) heated to ~ 250 °C (tri-acid solution), followed by a 3:1 mixture of sulphuric acid and hydrogen peroxide (Piranha solution) pre-heated to 90 °C. Silicon ions ($^{28}\text{Si}^+$) were then implanted into the sample with a dose of 10^{11} ions/cm^2 and an energy of 150 keV by Innovion Corporation. Note that the samples were purchased and implanted over the course of one year i.e. not in the same runs. The implantation energy was predicted to result in an implantation depth of 120 nm according to SRIM (Stopping and Range of Ions in Matter) simulations [41]. Subsequently, the samples were cleaned again using the tri-acid solution and then annealed for 12 hours at temperatures up to 1100 °C and under vacuum ($<10^{-6}$ torr) [15], followed by another tri-acid cleaning step.

Before investigating the effect of nanofabrication on the SiV properties, we characterized SiVs created in the bulk samples by implantation and annealing. The relevant electronic level structure of the SiV is shown in Fig. 1. It is composed of the ground ($^2\text{E}_g$) and excited state ($^2\text{E}_u$). For both, the spin-orbit interaction partially lifts their degeneracy and splits the states into the levels g_1, g_2 and e_1, e_2, respectively. Each of those levels further splits under the application of a magnetic field. The SiV features an optical transition at 737 nm (red arrow in Fig. 1) that we used for our experiments. The diamond sample was cooled to 5 K using a Montana Instruments closed cycle cryostat (Nanoscale Workstation). A standard homebuilt confocal microscope, described in [42], was employed for spectroscopic measurements: a long-working-distance microscope objective (NA = 0.5) was positioned outside the cyrostat using a three axis piezo stage to focus the excitation sources through the cyrostat top window and onto the sample surface. A single mode fiber was used as a pinhole to spatially filter the collected photoluminescence. This confocal microscope focused the green laser to a spot size of about 1 μm (full width half max) and always excited several color centers at the same time for the implantation density used here. Thus, all of our bulk spectra reflect inhomogeneous broadening of multiple illuminated SiV.

Optical Materials EXPRESS

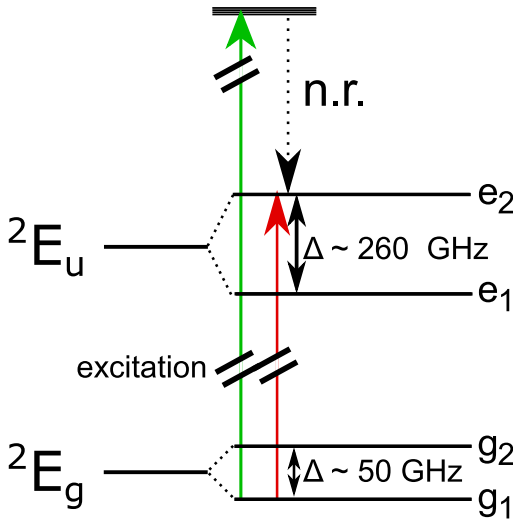

Fig. 1. Relevant energy-level structure of the negatively charged SiV. Off-resonant excitation (green arrow) populates the excited levels e_1 and e_2 via non radiative (n.r.) decays. Resonant excitation is represented by a red arrow.

As a first step in SiV characterization, we excited the samples incoherently with a 532 nm green laser (green arrow in Fig. 1) and monitored the emission using a spectrometer (Acton SP2750). Spectra from three different diamond chips, all produced with the same method, are shown in Fig. 2. Each spectrum shows peaks corresponding to the four expected optical transition lines connecting the two excited states with the two ground states. However, only Sample 3 (represented by the black trace) features inhomogeneous broadening narrow enough for each individual line to be clearly resolvable. The resolution of the spectrometer ($\approx$ 20 GHz) was not sufficient to resolve the contributions of individual SiV to the inhomogeneous broadening. To obtain high-resolution spectra, we scanned a tunable diode laser (New Focus Velocity TLB-6700) with a linewidth of around 1 MHz across the 737 nm absorption line, and monitored the photoluminescence from the phonon sideband (750-805 nm) [34]. An excerpt of the high-resolution spectrum together with the corresponding part of the low-resolution spectrum from the spectrometer is shown in the inset of Fig. 2. Note that in general the orientations of the implanted SiV are not expected to be aligned. As a result, some SiV will emit more efficiently into the nanopillar and microscope objective.

The spectrum from Sample 3 clearly shows contributions from SiVs with different emission wavelengths, likely due to each center experiencing a slightly different crystal environment in terms of residual stress from crystal polishing or implantation (i.e. the line is inhomogeneously broadened). bsphackesphack Since small inhomogeneous broadening is a key figure of merit, we investigated to what degree re-annealing the samples can relieve residual stress and reduce the inhomogeneous broadening of the centers. Re-annealing has been shown to reduce inhomogeneous broadening related to nanofabrication, for example [15,43]. Sample 1 (see Fig. 2) was re-annealed in a home-built vacuum tube furnace ($<10^{-6}$ Torr). The furnace temperature was increased from 20-800 °C over 6 hours, held at 800 °C for 4 hours, ramped to 1100 °C in 4 hours, and held at 1100 °C for 12 hours. Figure 3 shows the inhomogeneous broadening, averaged over measurements taken from many different spots on the sample, before annealing (red trace) and after annealing (blue trace). There is no observable difference between the spectra before and after re-annealing. bsphackesphack This indicates that individual sample properties may be influencing the degree of inhomogeneous broadening of the implanted SiV color centers.

Optical Materials EXPRESS

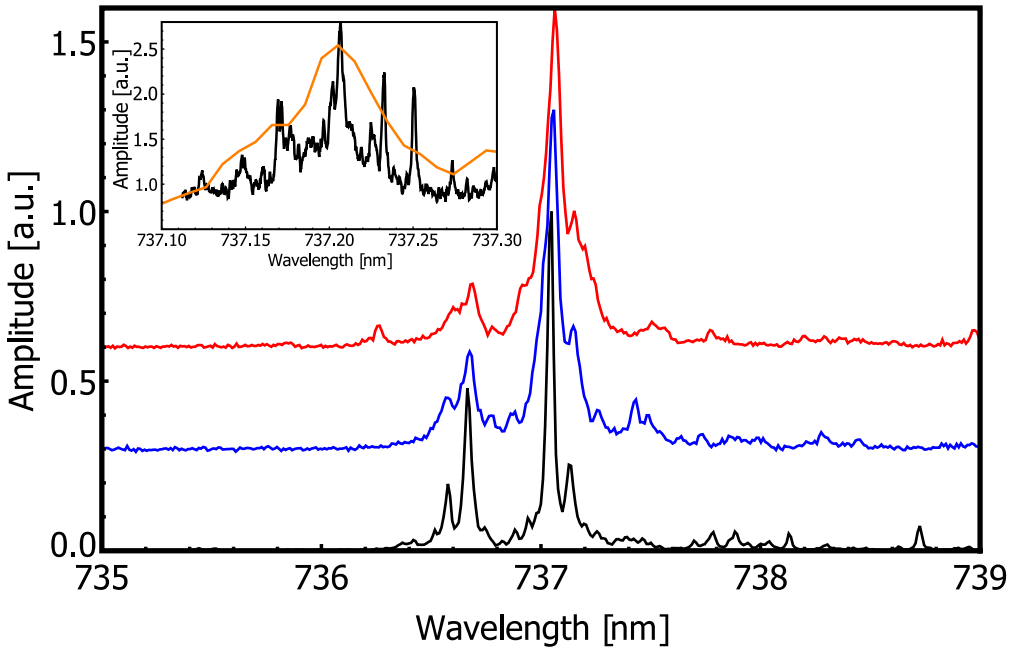

Fig. 2. Comparison of fluorescence emission spectra (532 nm excitation) of SiV ensembles created via implantation and annealing in different diamond chips under the same conditions. Black trace: Sample 3, blue trace: Sample 1, red trace: Sample 2. Inset: Comparison of a resonant excitation photoluminescence scan and lower-resolution fluorescence spectrum under off-resonant excitation for Sample 3.

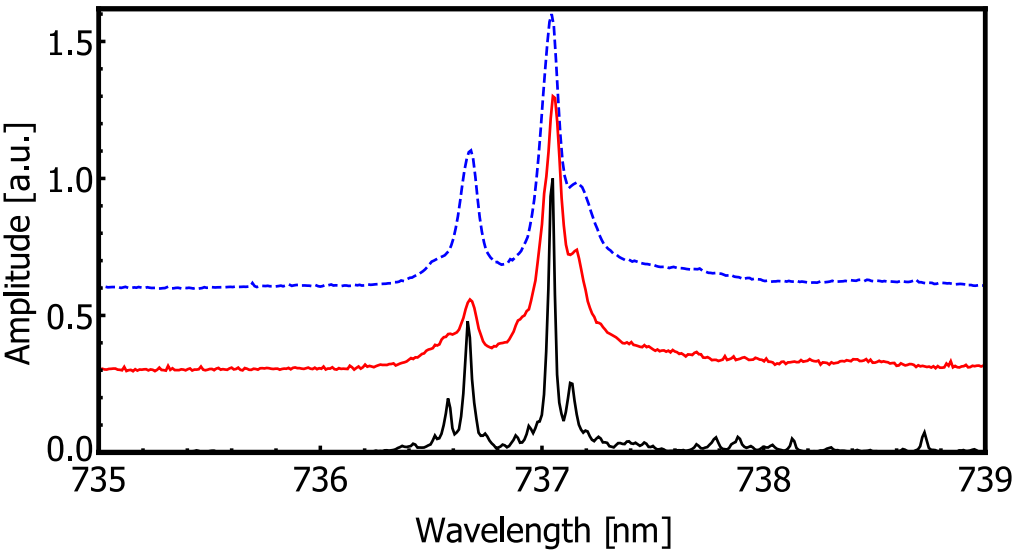

Fig. 3. High resolution resonant excitation photoluminescence measurements of implanted SiVs, comparing the inhomogeneous broadening in Sample 1 before (red trace) and after additional annealing (blue trace) for 12 hours at 1100 °C and under vacuum ($<10^{-6}$ Torr). For reference, the spectrum of Sample 3 showing the inhomogeneous broadening without additional annealing (black trace) is also shown.

Optical Materials EXPRESS

As mentioned above, one possible source of the observed differences in optical properties is variation between each sample's internal stress. The impact of diamond polishing on color center properties has been shown in previous studies to be significant [44–47]. Pre-etching the surface, i.e. removal of the top layer of potentially damaged or stressed diamond by reactive ion etching, has been shown to improve color center properties [44,46]. This was used for sample 2 that exhibited poor inhomogeneous broadening, indicating that either the pre-etch was not sufficiently deep or that surface damage and stress is not responsible for the observed behaviour. Sample processing, such as cleaning, implantation, and annealing could also in principle vary from sample to sample as it was executed at different times for each sample. However, the fact that repeated annealing and cleaning was not observed to improve SiV sample properties in samples with poor inhomogeneous broadening, suggests that these steps are not responsible for the observed variations. bsphackesphack In future, additional pre-etching [46] and annealing at higher temperatures and higher vacuum as in [43,48] can be investigated to improve the repeatability of obtaining SiV emitters with low inhomogeneous broadening. In addition, techniques for reducing inhomogeneous broadening through blue laser excitation may also improve the spectral properties of the implanted SiVs, as observed in [43].

3. Effect of etched nanopillars on SiV spin lifetime

For applications involving color centers embedded within nanostructures, it is valuable to understand how their properties are affected by the nanofabrication process and the fabricated nanostructure geometry. This is particularly interesting for the coupling of color centers to photonic or phononic nanocavities, where predicted enhancements of the color center's spin dynamics from locally engineered density of states [20,39] can be degraded by etched surfaces and other nanofabrication-induced changes to the material. Ideally, such changes can be minimized through optimized processing, for example by using gentle etching processes [49] and surface treatments [44,50]. To investigate how nanofabrication, and in particular surfaces created using oxygen plasma etching, influences SiV properties, we conducted a study of the lifetime of the upper orbital state (labeled g_2 in Fig. 1) of the negatively charged SiV ground state manifold. These measurements were conducted for SiV color centers in nanostructures with varying dimension, as described below. We performed these experiments on Sample 3, which showed the smallest inhomogeneous broadening in the characterization experiments described above.

The pattern used here to probe the influence of nanofabrication on SiV spin lifetime was an array of nanopillars with diameters varying from 120 to 900 nm. The nanopillars were created using electron beam lithography followed by C_4F_8/SF_6 reactive ion etching to transfer the nanopillar array pattern to a silicon nitride hard mask deposited on the diamond chip using plasma enhanced chemical vapour deposition (PECVD). An oxygen plasma etch was then used to transfer the pattern to the diamond chip. The etched nanopillars have height of ~ 1000 nm. We followed the same process as described in [51] omitting only the final isotropic undercutting steps which were not required for these nanopillar structures. After etching, the sample was cleaned in hydrofluoric acid solution to remove the SiN, followed by tri-acid and Piranha cleaning solutions. A scanning electron microscope image of the resulting nanopillars is shown in Fig. 4.

To measure the lifetimes of the upper orbital state $|g_2\rangle$ of implanted SiVs in the nanopillars, we optically excited the SiV resonantly on the $|g_i\rangle \rightarrow |e_i\rangle$ $(i = 1, 2)$ transitions and monitored the resulting phonon sideband fluorescence as in the resonant excitation measurements from Fig. 2. We first transfered population from the ground state $|g_1\rangle$ into the upper orbital state via the application of a laser pulse resonant with the transition $|g_1\rangle \rightarrow |e_2\rangle$, which then decayed into either orbital ground state. By pumping long enough (~ 80 ns), most population was transferred to state $|g_2\rangle$. Due to this population inversion, the fluorescence collected and measured with an avalanche photodiode decreased during the excitation pulse. To extract the lifetime of the $|g_2\rangle$ state, another 80 ns pulse was applied on the same transition after a wait time τ. Depending

Optical Materials EXPRESS

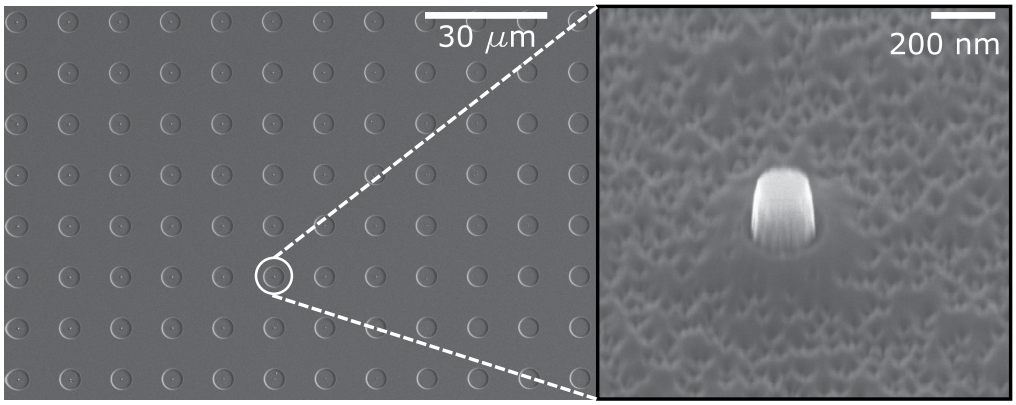

Fig. 4. Scanning electron microscope images of the fabricated nanopillars. The inset image shows a 225 nm diameter nanopillar.

on the wait time and the lifetime of the orbital state, some population relaxed back into ground state $|g_1\rangle$, which manifested itself in an increase in fluorescence compared to the steady state fluorescence at the end of the first pulse. The lifetime T_1 could then be extracted by fitting an exponential function

$$\frac{A_1}{A_2}(\tau) = 1 + A \exp\left(-\frac{\tau}{T_1}\right) \tag{1}$$

to the ratio of the integrated fluorescence signal during first population inversion pulse A_1 and the second population inversion (readout) pulse A_2. Here A is the maximum observed population inversion fraction. An example spin lifetime measurement of an SiV in a 300 nm nanopillar is shown in the inset of Fig. 5(a). Note that under resonant excitation the SiV can change its charge state and subsequently turn dark. However, it is possible to reset an SiV to the negative charge state using excitation at 532 nm [52,53]. Therefore for every 1000 iterations of the lifetime measurement ($1000 \times 2 \times 80$ ns, 37 μW, 737 nm cw power) we applied a charge state reset green laser pulse (45 us, 20 μW 532 nm cw power).

Using this method, we measured the orbital state lifetime of implanted SiVs in nanopillars of varying diameter and compared it to the result obtained for SiVs in unpatterned regions of the same chip far from the fabricated nanopillars. The lifetime of the upper orbital state and its dependence on the nanopillar diameter is shown in Fig. 5(a) where the bulk lifetime with an uncertainty of ± 4 ns (due to the averaging of SiVs in different locations within the bulk) is represented as a horizontal line. Note that ground state splitting of typical SiV lines measured here is <0.1 nm (57 GHz), as shown in Fig. 2. The spin lifetime of these color centers is not expected to be enhanced by residual strain, unlike spins with large (>100 GHz) splitting studied in Ref. [36].

For SiVs in bulk diamond the lifetime of $|g_2\rangle$ is limited by vibrational modes (phonons) [34,54] resonant with the transition to the ground state $|g_1\rangle$. At low temperature, spin lifetime is expected to vary inversely with density of states [36], and in small structures the density of these modes is expected to decrease [20,39]. Building upon simulations of spherical nanoparticles and phononic crystals in Ref. [20], simulations of the phononic density of states of nanopillars illustrated in Fig. 5(b) were performed using COMSOL finite element simulation software. The resulting predicted density of states for nanopillars with diameters 150 nm, 300 nm and 400 nm are shown in Fig. 5(c). These simulations predict that for the 50 GHz splitting of the two orbital states $|g_{1,2}\rangle$ studied here, resonant phonons should be restricted–frozen out–in structures with dimensions smaller than ≈ 150 nm. Such a restriction is expected to manifest itself in an increase in the

Optical Materials EXPRESS

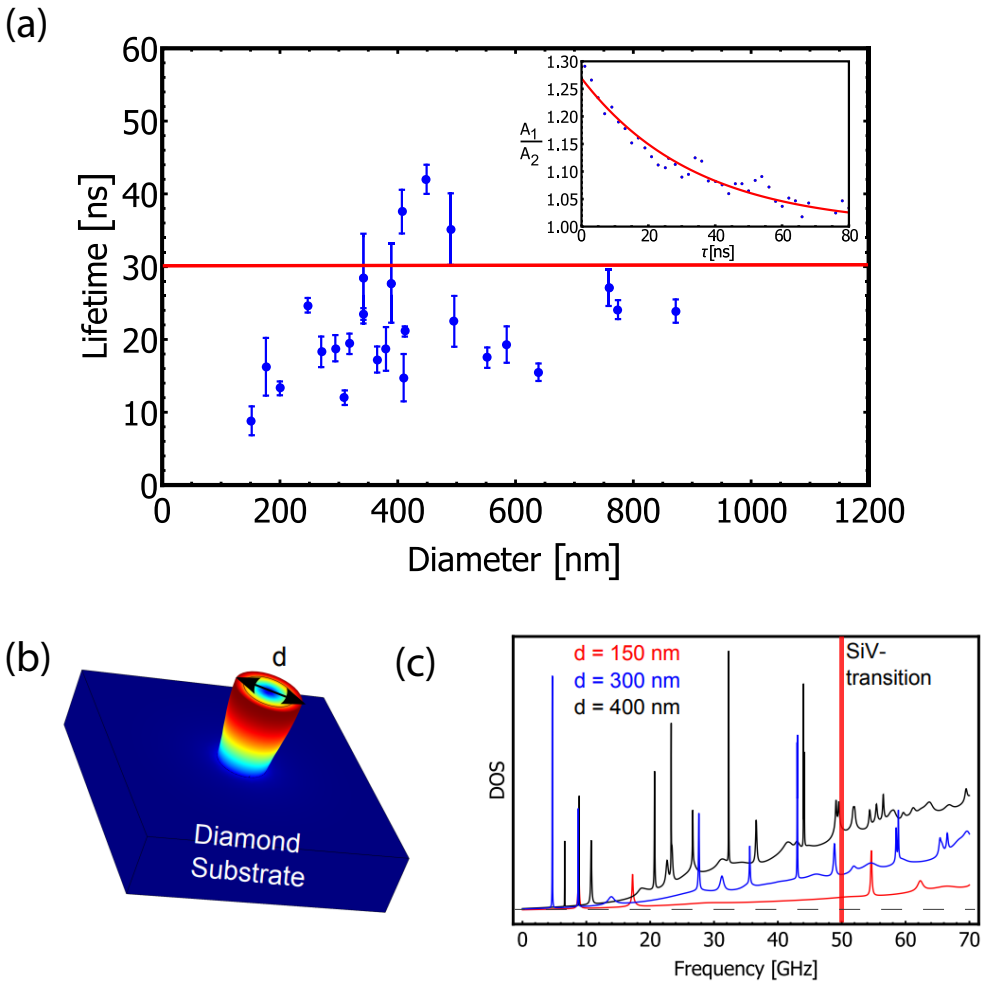

Fig. 5. (a) Orbital state lifetime of SiV centers in nanopillars of different diameters. Experimental data is displayed as blue dots. Each dot is an average over several nanopillars with the errorbar corresponding to the standard deviation of the measurements. The horizontal red line, with an uncertainty (shaded region) of ± 4 ns between individual centers, indicates the orbital state lifetime of SiV in unpatterned regions of the chip. Inset: Example decay of the population ratio A_1/A_2 of an SiV in a 300 nm nanopillar. (b) Simulated nanopillar geometery. Pillar height is 1 μm and diameter d varies. (c) Simulated nanopillar phonon density of states. Dashed line is a guide to the eye to show the increase in density of state background as frequency increases.

Optical Materials EXPRESS

orbital state lifetime. However, note that coupling between nanopillar modes and the continuum of bulk substrate modes visible as a background in the density of states simulations in Fig. 5(c) could degrade the effect of the suppression of discrete localized nanopillar mechanical modes.

Our measurements show that the largest nanopillars possess lifetimes comparable to the bulk. In smaller nanopillars with diameters around 500 nm, some SiVs exhibit slightly longer lifetimes than the bulk average. This may indeed be a weak signature of an onset of the expected lifetime increase in small structures. However, overall our lifetime measurements show a strong scatter with a decreasing trend for smaller nanopillar sizes. The strong scatter may stem from the fact that the measured SiV were not always in the nanopillar's center since our nanopillars were fabricated after SiV implantation without first determining the location of individual SiVs. An SiV located near the edge of a large nanopillar where the crystal lattice is imperfect can thus possess a lifetime bsphackesphack that deviates from its nominally predicted value. Reduced lifetimes may be caused by imperfections in the crystal lattice surrounding the SiV, likely created during etching [15,43]. Studies by Evans et al. [15] and Zuber et al. [43] have shown that post-fabrication annealing may improve the SiV properties. Additionally, broadening of the phononic modes of the nanopillar due to mechanical loss not captured by the density of states simulations due to imperfect fabrication or material properties, in addition to the influence of the background in the density of states calculations in Fig. 5(c), may reduce the impact of the expected modification to the phononic density of states on the SiV spin dynamics. Such effects have recently been observed in diamond nanowires, whose small nominal density of states was found to not affect the dynamics of SiV spins [38]. To bsphackesphack further test our hypothesis that restricted vibrational modes can extend lifetimes, more data, especially from centers that are deterministically placed in high-quality, small diameter nanopillars bsphackesphack are needed.

4. Conclusion

The experiments described in this manuscript demonstrate the impact of both diamond sample choice and nanofabrication on the optical and spin properties of SiV color centers. Despite working with nominally identical samples, significant variations in inhomogeneous broadening of SiVs created by implantation and annealing were observed. One sample was observed to possess a narrow enough inhomogeneous broadening to resolve the four lines of the SiV, and re-annealing was not found to be successful in influencing the inhomogeneous linewidth. Using a sample with low inhomogeneous broadening, we found that the orbital state lifetime can be affected by nanofabrication. For some SiVs in nanopillars with diameters around 500 nm we find slightly increased lifetimes compared to the bulk that may be due to restriction of vibrational modes. However, the measured lifetimes show strong scatter, presumably due to random placement of SiVs within the nanopillars, and for the smallest structures we found a trend towards decreased lifetimes. This may be due to imperfections in the crystal lattice or surface damage caused by etching, which can affect the dynamics of diamond spin systems [46] and quantum dots [55]. We note that a recent study by Kuruma et al. [38] found that diamond nanowires, which like the nanopillars studied here offer reduced phononic density of states but lack a complete phononic bandgap at the SiV spin transition frequency, have no effect on SiV spin lifetimes. This suggests that phonon leakage into these structures plays a large role in governing the spin state dynamics. It is also possible that variations in the nanopillar effective phononic density of states as a function of position could affect the spin lifetime.

To confirm an increase in orbital state lifetime due to the suppression of vibrational modes, more experiments with deterministically placed SiVs in high-quality nanopillars with sizes below 500 nm [18] are needed. Simulations of the position dependence of the phononic density of states may provide insight into the positioning resolution required for SiVs to be robustly affected by the phonon restriction effects predicted by Lutz et al. for nanopillars as well as phononic crystals [20].

Optical Materials EXPRESS

Funding. European Commission Recovery and Resilience Facility (2.3.1.1.i.0/1/22/I/CFLA/001); Natural Sciences and Engineering Research Council of Canada; Alberta Innovates; Canada Foundation for Innovation; Canadian Institute for Advanced Research.

Disclosures. The authors declare no conflicts of interest.

Data availability. Data underlying the results presented in this paper are not publicly available at this time but may be obtained from the authors upon reasonable request.

References

1. J. R. Maze, P. L. Stanwix, J. S. Hodges, *et al.*, "Nanoscale magnetic sensing with an individual electronic spin in diamond," Nature **455**(7213), 644–647 (2008).
2. C. Degen, F. Reinhard, and P. Cappellaro, "Quantum sensing," Rev. Mod. Phys. **89**(3), 035002 (2017).
3. M. J. Burek, J. D. Cohen, S. M. Meenehan, *et al.*, "Diamond optomechanical crystals," Optica **3**(12), 1404–1411 (2016).
4. D. A. Golter, T. Oo, M. Amezcua, *et al.*, "Optomechanical quantum control of a nitrogen-vacancy center in diamond," Phys. Rev. Lett. **116**(14), 143602 (2016).
5. D. Lee, K. W. Lee, J. V. Cady, *et al.*, "Topical review: spins and mechanics in diamond," J. Opt. **19**(3), 033001 (2017).
6. P. K. Shandilya, S. Flagan, N. C. Carvalho, *et al.*, "Diamond integrated quantum nanophotonics: Spins, photons and phonons," J. Lightwave Technol. **40**(23), 7538–7571 (2022).
7. F. Jelezko, T. Gaebel, I. Popa, *et al.*, "Observation of coherent oscillation of a single nuclear spin and realization of a two-qubit conditional quantum gate," Phys. Rev. Lett. **93**(13), 130501 (2004).
8. M. G. Dutt, L. Childress, L. Jiang, *et al.*, "Quantum register based on individual electronic and nuclear spin qubits in diamond," Science **316**(5829), 1312–1316 (2007).
9. G. D. Fuchs, G. Burkard, P. V. Klimov, *et al.*, "A quantum memory intrinsic to single nitrogen-vacancy centres in diamond," Nat. Phys. **7**(10), 789–793 (2011).
10. B. Hensen, H. Bernien, A. E. Dréau, *et al.*, "Loophole-free bell inequality violation using electron spins separated by 1.3 kilometres," Nature **526**(7575), 682–686 (2015).
11. L. Childress and R. Hanson, "Diamond nv centers for quantum computing and quantum networks," MRS Bull. **38**(2), 134–138 (2013).
12. M. Atatüre, D. Englund, N. Vamivakas, *et al.*, "Material platforms for spin-based photonic quantum technologies," Nat. Rev. Mater. **3**(5), 38–51 (2018).
13. M. Salz, Y. Herrmann, A. Nadarajah, *et al.*, "Cryogenic platform for coupling color centers in diamond membranes to a fiberbased microcavity," Appl. Phys. B **126**, 131 (2020).
14. E. Janitz, M. K. Bhaskar, and L. Childress, "Cavity quantum electrodynamics with color centers in diamond," Optica **7**(10), 1232–1252 (2020).
15. R. E. Evans, A. Sipahigil, D. D. Sukachev, *et al.*, "Narrow-linewidth homogeneous optical emitters in diamond nanostructures via silicon ion implantation," Phys. Rev. Appl. **5**(4), 044010 (2016).
16. P. Kehayias, A. Jarmola, N. Mosavian, *et al.*, "Solution nuclear magnetic resonance spectroscopy on a nanostructured diamond chip," Nat. Commun. **8**(1), 188 (2017).
17. T. Schröder, S. L. Mouradian, J. Zheng, *et al.*, "Quantum nanophotonics in diamond," J. Opt. Soc. Am. B **33**(4), B65–B83 (2016).
18. J. L. Zhang, K. G. Lagoudakis, Y.-K. Tzeng, *et al.*, "Complete coherent control of silicon vacancies in diamond nanopillars containing single defect centers," Optica **4**(11), 1317 (2017).
19. M. Fujita, S. Takahashi, Y. Tanaka, *et al.*, "Simultaneous inhibition and redistribution of spontaneous light emission in photonic crystals," Science **308**(5726), 1296–1298 (2005).
20. T. Lutz, L. Veissier, C. W. Thiel, *et al.*, "Modification of phonon processes in nanostructured rare-earth-ion-doped crystals," Phys. Rev. A **94**(1), 013801 (2016).
21. A. Sipahigil, K. D. Jahnke, L. J. Rogers, *et al.*, "Indistinguishable photons from separated silicon-vacancy centers in diamond," Phys. Rev. Lett. **113**(11), 113602 (2014).
22. L. Marseglia, K. Saha, A. Ajoy, *et al.*, "Bright nanowire single photon source based on SiV centers in diamond," Opt. Express **26**(1), 80–89 (2018).
23. C. Weinzetl, J. Görlitz, J. N. Becker, *et al.*, "Coherent control and wave mixing in an ensemble of silicon-vacancy centers in diamond," Phys. Rev. Lett. **122**(6), 063601 (2019).
24. A. Sipahigil, R. E. Evans, D. D. Sukachev, *et al.*, "An integrated diamond nanophotonics platform for quantum-optical networks," Science **354**(6314), 847–850 (2016).
25. Y.-I. Sohn, S. Meesala, B. Pingault, *et al.*, "Controlling the coherence of a diamond spin qubit through its strain environment," Nat. Commun. **9**(1), 2012 (2018).
26. S. Wein, N. Lauk, R. Ghobadi, *et al.*, "Feasibility of efficient room-temperature solid-state sources of indistinguishable single photons using ultrasmall mode volume cavities," Phys. Rev. B **97**(20), 205418 (2018).
27. S. Maity, L. Shao, S. Bogdanovic, *et al.*, "Coherent acoustic control of a single silicon vacancy spin in diamond," Nat. Commun. **11**, 193(2019).

Optical Materials EXPRESS

28. C. T. Nguyen, D. D. Sukachev, M. K. Bhaskar, *et al.*, "An integrated nanophotonic quantum register based on silicon-vacancy spins in diamond," Phys. Rev. B **100**, 165428 (2019).
29. Y. Silani, F. Hubert, and V. M. Acosta, "Stimulated emission depletion microscopy with diamond silicon vacancy centers," ACS Photonics **6**(10), 2577–2582 (2019).
30. P.-J. Stas, Y. Q. Huan, B. Machielse, *et al.*, "Robust multi-qubit quantum network node with integrated error detection," Science **378**(6619), 557–560 (2022).
31. E. Bersin, M. Sutula, Y. Q. Huan, *et al.*, "Telecom networking with a diamond quantum memory," Accepted to Phys. Rev. J. (2023).
32. J. N. Becker, B. Pingault, D. Groß, *et al.*, "All-optical control of the silicon-vacancy spin in diamond at millikelvin temperatures," Phys. Rev. Lett. **120**(5), 053603 (2018).
33. E. Neu, D. Steinmetz, J. Riedrich-Möller, *et al.*, "Single photon emission from silicon-vacancy colour centres in chemical vapour deposition nano-diamonds on iridium," New J. Phys. **13**(2), 025012 (2011).
34. K. D. Jahnke, A. Sipahigil, J. M. Binder, *et al.*, "Electron–phonon processes of the silicon-vacancy centre in diamond," New J. Phys. **17**(4), 043011 (2015).
35. D. Sukachev, A. Sipahigil, C. Nguyen, *et al.*, "Silicon-vacancy spin qubit in diamond: A quantum memory exceeding 10 ms with single-shot state readout," Phys. Rev. Lett. **119**(22), 223602 (2017).
36. S. Meesala, Y.-I. Sohn, B. Pingault, *et al.*, "Strain engineering of the silicon-vacancy center in diamond," Phys. Rev. B **97**(20), 205444 (2018).
37. K. Kurama, B. Pingault, C. Chia, *et al.*, "Extension of orbital lifetimes of silicon-vacancy centers in diamond using phononic crystals," Bulletin of the American Physical Society (2023).
38. K. Kuruma, B. Pingault, C. Chia, *et al.*, "Engineering phonon-qubit interactions using phononic crystals," arxiv, arxiv:2310.06236 (2023).
39. M. Klotz, K. Fehler, R. Waltrich, *et al.*, "Prolonged orbital relaxation by locally modified phonon density of states for the siv center in nanodiamonds," Phys. Rev. Lett. **128**(15), 153602 (2022).
40. A. E. Rugar, C. Dory, S. Sun, *et al.*, "Characterization of optical and spin properties of single tin-vacancy centers in diamond nanopillars," Phys. Rev. B **99**(20), 205417 (2019).
41. J. F. Ziegler, M. Ziegler, and J. Biersack, "Srim – the stopping and range of ions in matter (2010)," Nucl. Instruments Methods Phys. Res. Sect. B: Beam Interactions with Mater. Atoms **268**(11-12), 1818–1823 (2010). 19th International Conference on Ion Beam Analysis.
42. J. P. Hadden, V. Bharadwaj, B. Sotillo, *et al.*, "Integrated waveguides and deterministically positioned nitrogen vacancy centers in diamond created by femtosecond laser writing," Opt. Lett. **43**(15), 3586–3589 (2018).
43. J. A. Zuber, M. Li, M. l. G. Puigibert, *et al.*, "Shallow silicon vacancy centers with lifetime-limited optical linewidths in diamond nanostructures," Nano Lett. **23**, 10901 (2023).
44. Y. Chu, N. de Leon, B. Shields, *et al.*, "Coherent optical transitions in implanted nitrogen vacancy centers," Nano Lett. **14**(4), 1982–1986 (2014).
45. T. Lühmann, N. Raatz, R. John, *et al.*, "Screening and engineering of colour centres in diamond," J. Phys. D: Appl. Phys. **51**(48), 483002 (2018).
46. S. Sangtawesin, B. L. Dwyer, S. Srinivasan, *et al.*, "Origins of diamond surface noise probed by correlating single-spin measurements with surface spectroscopy," Phys. Rev. X **9**(3), 031052 (2019).
47. M. W. N. Ngambou, P. Perrin, I. Balasa, *et al.*, "Optimizing ion implantation to create shallow NV centre ensembles in high-quality CVD diamond," Mater. Quantum. Technol. **2**(4), 045001 (2022).
48. J. Lang, S. Häußler, J. Fuhrmann, *et al.*, "Long optical coherence times of shallow-implanted, negatively charged silicon vacancy centers in diamond," Appl. Phys. Lett. **116**(6), 1 (2020).
49. S. Cui, "Near-surface nitrogen vacancy centers in diamond," Ph.D. thesis, Harvard University (2014).
50. K.-M. C. Fu, C. Santori, P. E. Barclay, *et al.*, "Conversion of neutral nitrogen-vacancy centers to negatively charged nitrogen-vacancy centers through selective oxidation," Appl. Phys. Lett. **96**(12), 121907 (2010).
51. B. Khanaliloo, H. Jayakumar, A. C. Hryciw, *et al.*, "Single-crystal diamond nanobeam waveguide optomechanics," Phys. Rev. X **5**(4), 041051 (2015).
52. S. Dhomkar, P. R. Zangara, J. Henshaw, *et al.*, "On-demand generation of neutral and negatively charged silicon-vacancy centers in diamond," Phys. Rev. Lett. **120**(11), 117401 (2018).
53. L. Nicolas, T. Delord, P. Huillery, *et al.*, "Sub-ghz linewidth ensembles of siv centers in a diamond nano-pyramid obtained by persistent hole burning," arXiv, arXiv:1901.10853v2 (2019).
54. A. Liu and S. T. Cundiff, "Spectroscopic signatures of electron-phonon coupling in silicon-vacancy centers in diamond," Phys. Rev. Mater. **4**, 055202 (2020).
55. J. Liu, K. Konthasinghe, M. Davanço, *et al.*, "Single self-assembled quantum dots in photonic nanostructures: The role of nanofabrication," Phys. Rev. Appl. **9**(6), 064019 (2018).